Electronic Supplementary Information

A luminescent silver-phosphine tetragonal cage based on tetraphenylethylene

Juan Feng, Liu Yao, Jianyong Zhang,* Yingxiao Mu, Zhenguo Chi and Cheng-Yong Su

MOE Laboratory of Bioinorganic and Synthetic Chemistry, Lehn Institute of Functional Materials, School of Chemistry and Chemical Engineering, Sun Yat-Sen University, Guangzhou 510275, China. Email: zhjyong@mail.sysu.edu.cn

Table S1 Fluorescence lifetime data of L and Ag_4L_2 in solution and in solid state. (The resulting signals were fitted with a double exponential decay function, which obtained the best fit with respect to both the recorded phase and intensity information.)

	Sample	τ_1/ns[a]	A_1[b]	τ_2/ns[a]	A_2[b]	$<\tau>$/ns[c]
L	in $CHCl_3$ (3.64×10^{-5} mol L^{-1})	0.30	0.66	3.08	0.34	1.25
	solid	2.84	0.55	6.13	0.45	4.32
Ag_4L_2	in $CHCl_3$ (1.42×10^{-5} mol L^{-1})	1.24	0.22	2.93	0.78	2.56
	solid	2.10	0.40	3.89	0.60	3.17

[a] Fluorescence lifetime. [b] Fractional contribution. [c] Weighted mean lifetime $<\tau> = \frac{A_1\tau_1 + A_2\tau_2}{A_1+A_2}$.

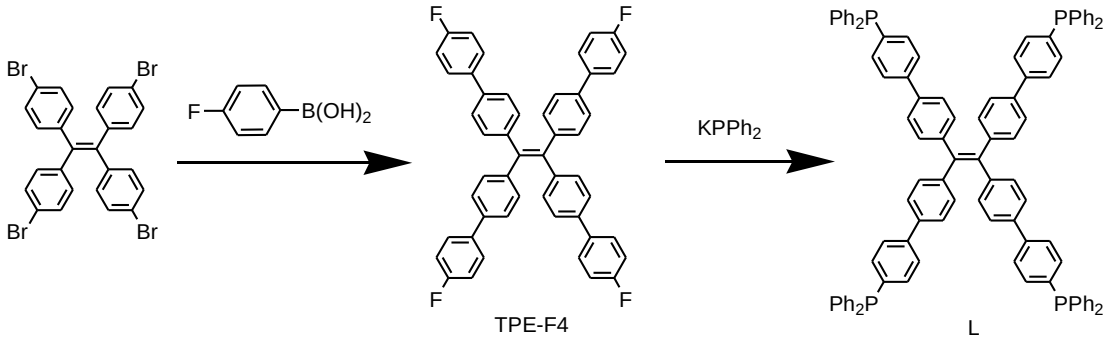

Scheme S1 Synthetic route for 1,1,2,2-tetrakis(4-diphenylphosphino-(1,1'-biphenyl))ethane (L).

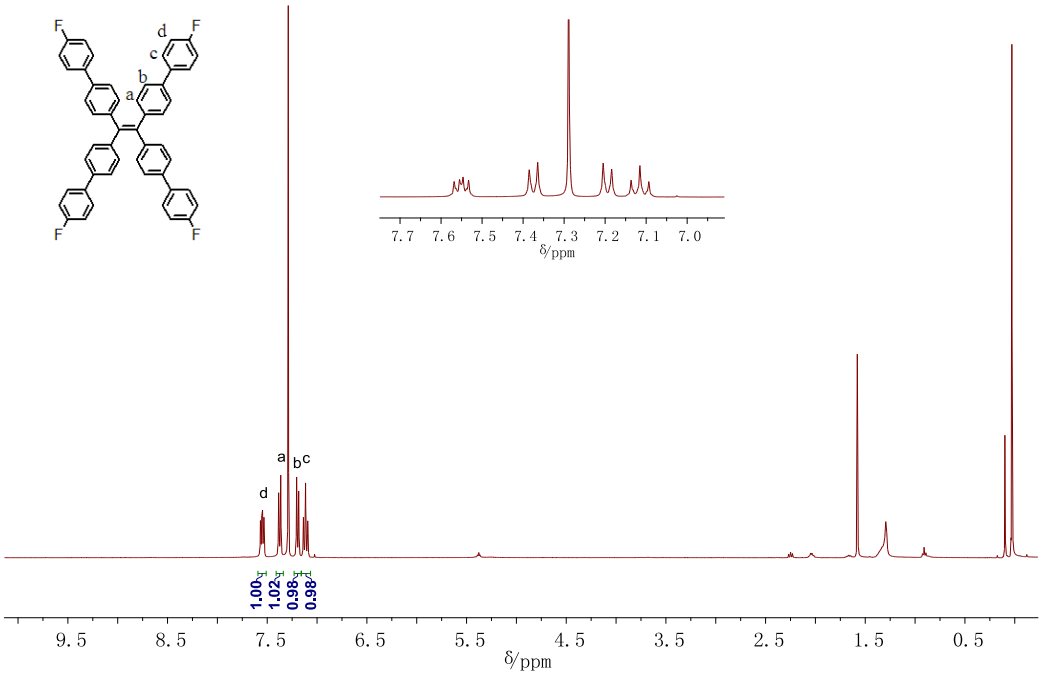

Fig. S1 ^{1}H NMR spectrum (400 MHz, $CDCl_3$) of TPE-F4.

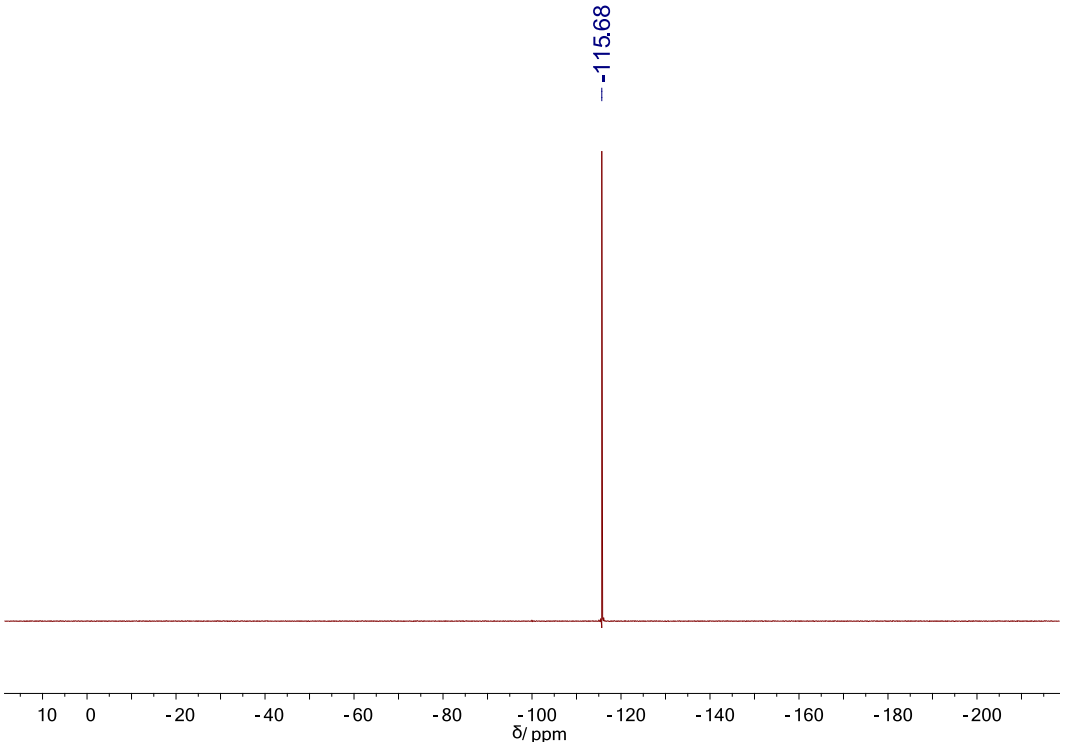

Fig. S2 ^{19}F NMR spectrum (377 MHz, $CDCl_3$) of TPE-F4.

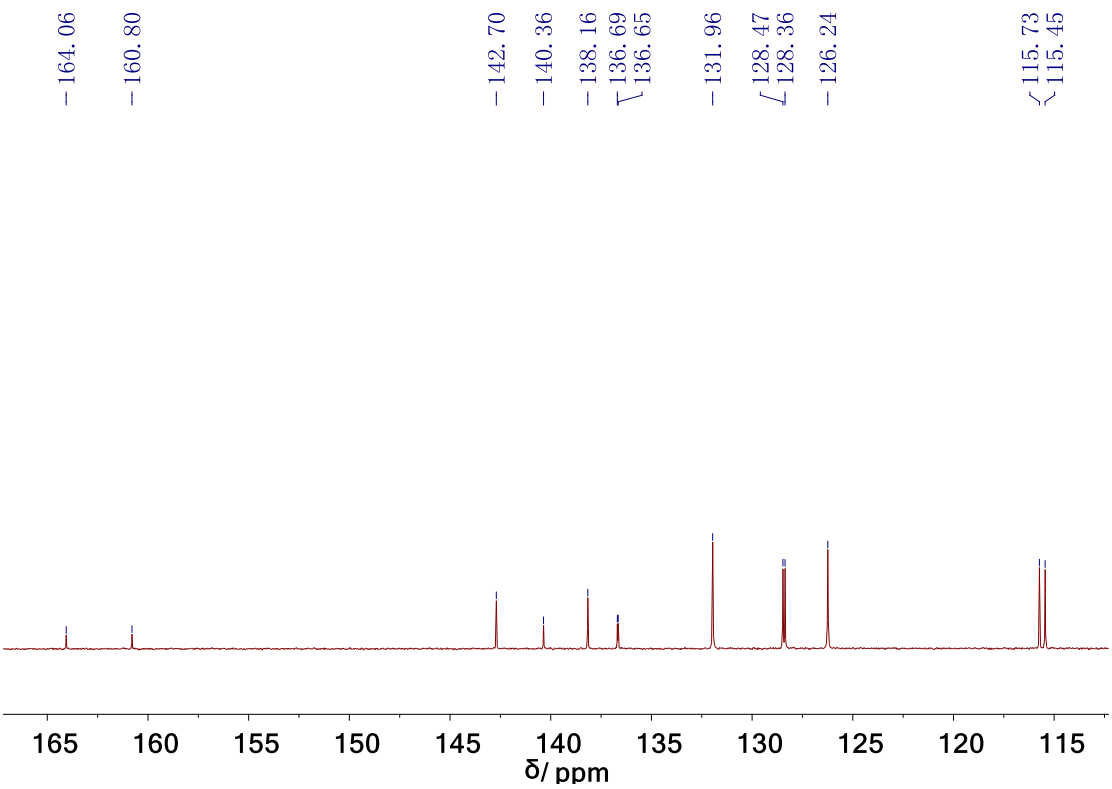

Fig. S3 ^{13}C NMR spectrum ($CDCl_3$, 75 MHz) of TPE-F4.

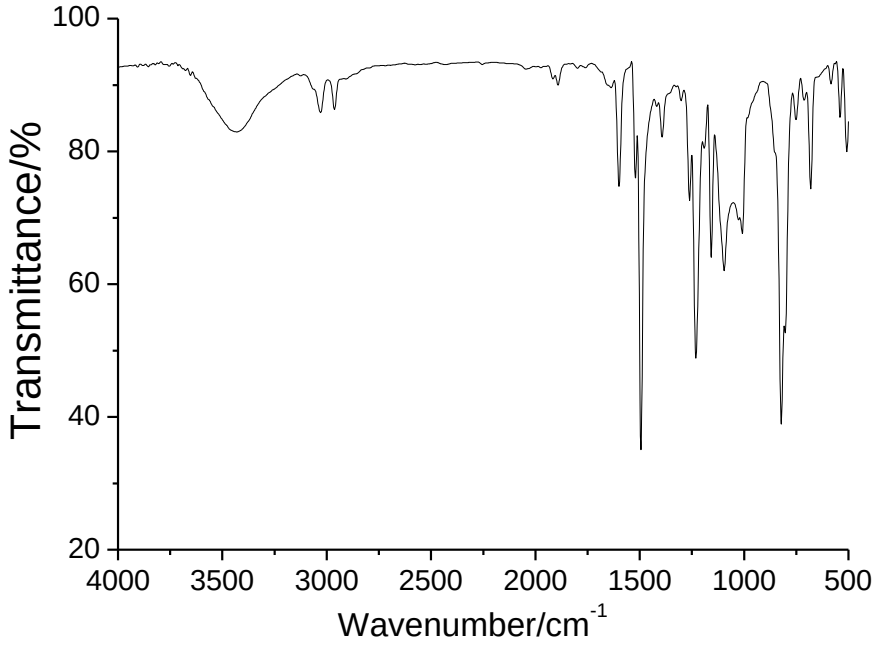

Fig. S4 FT-IR spectrum of TPE-F4 (KBr pellets).

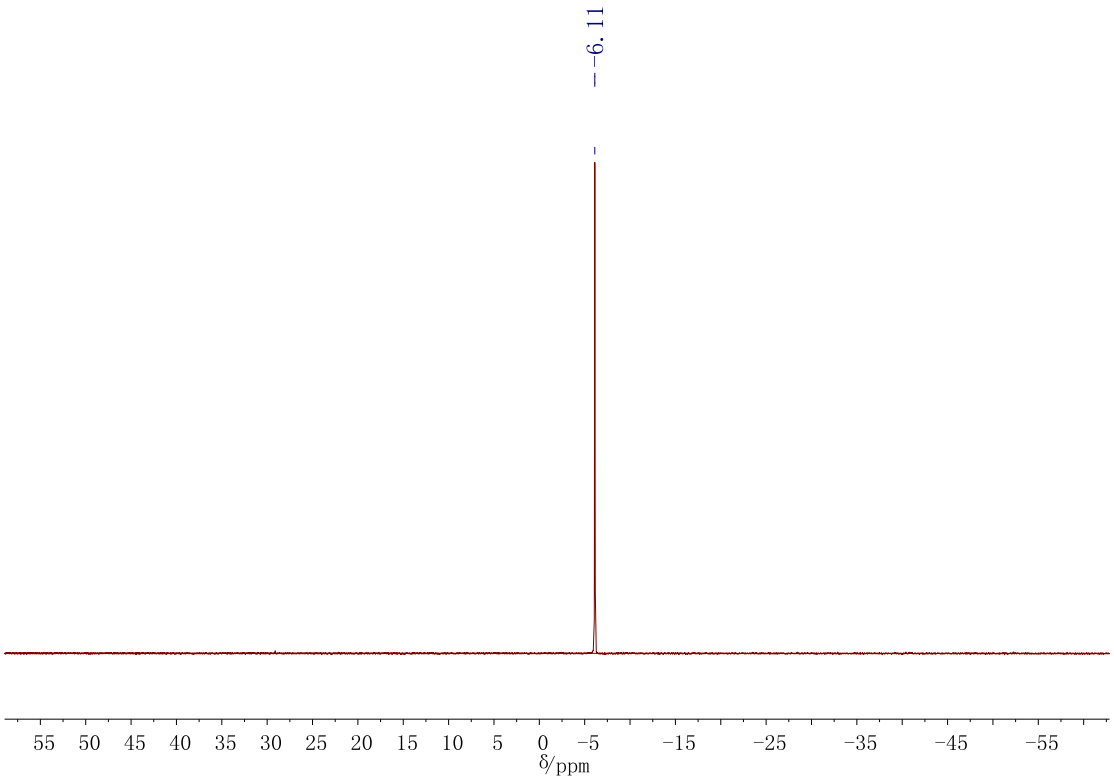

Fig. S5 $^{31}P\{^{1}H\}$ NMR spectrum ($CDCl_3$, 162 MHz) of L.

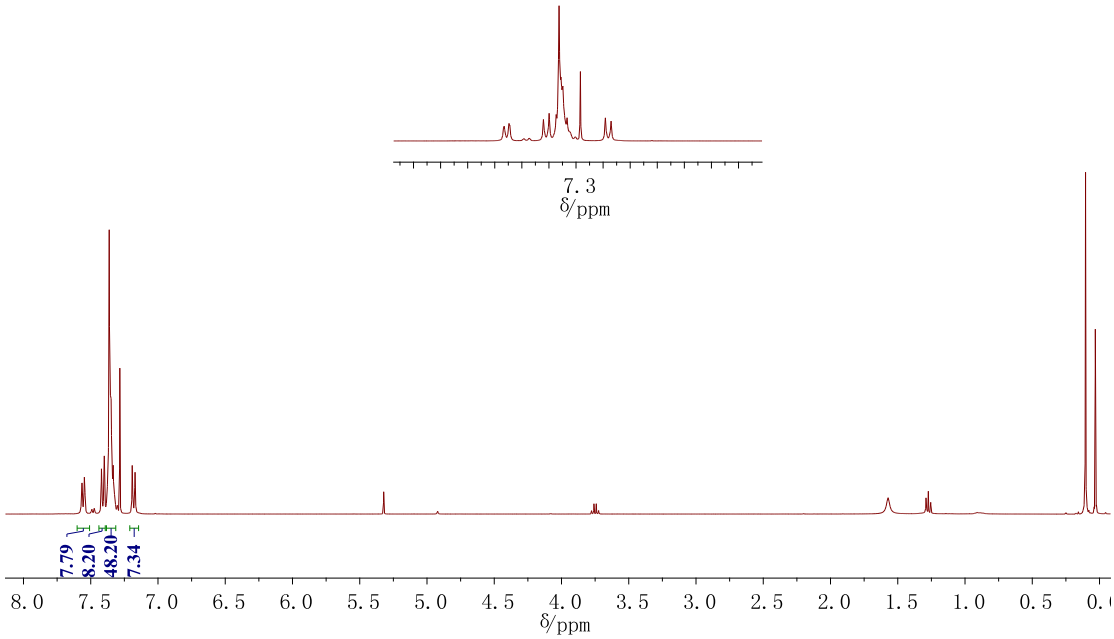

Fig. S6 ^{1}H NMR spectrum ($CDCl_3$, 400 MHz) of L.

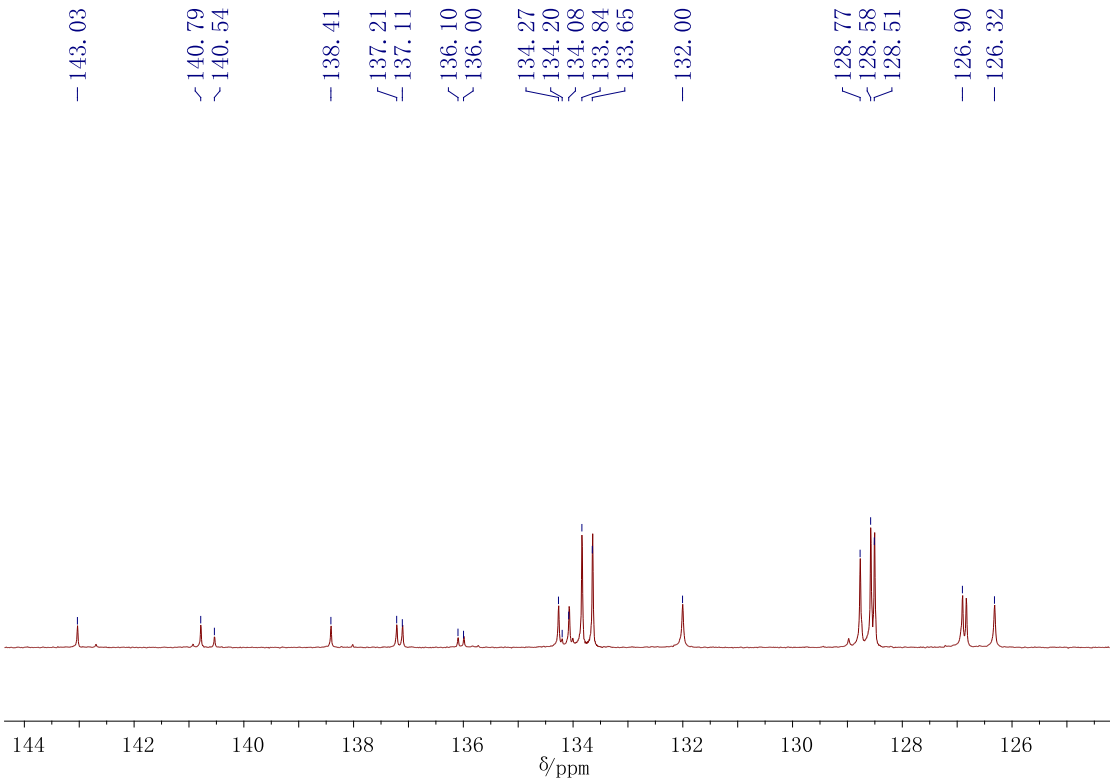

Fig. S7 ^{13}C NMR spectrum ($CDCl_3$, 101 MHz) of L.

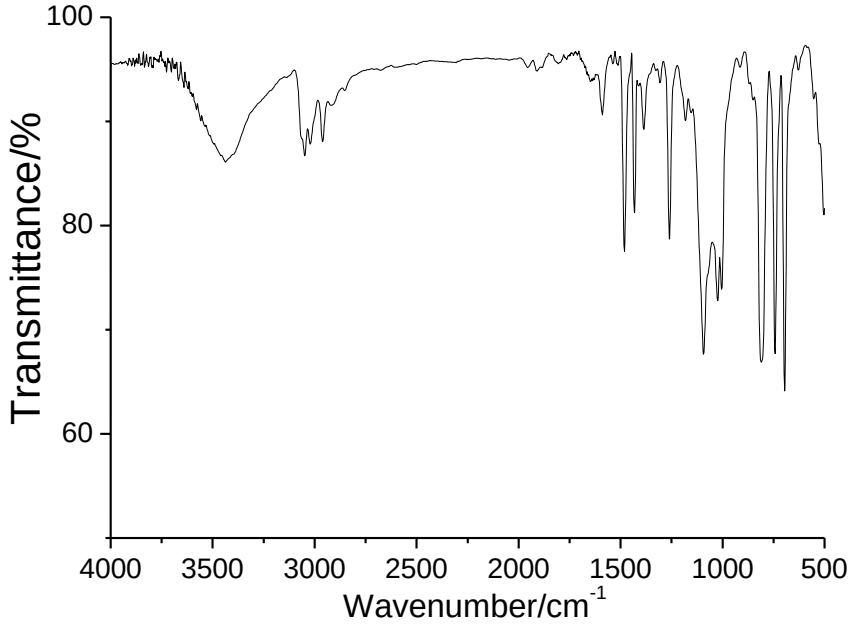

Fig. S8 FT-IR spectrum of L (KBr pellets).

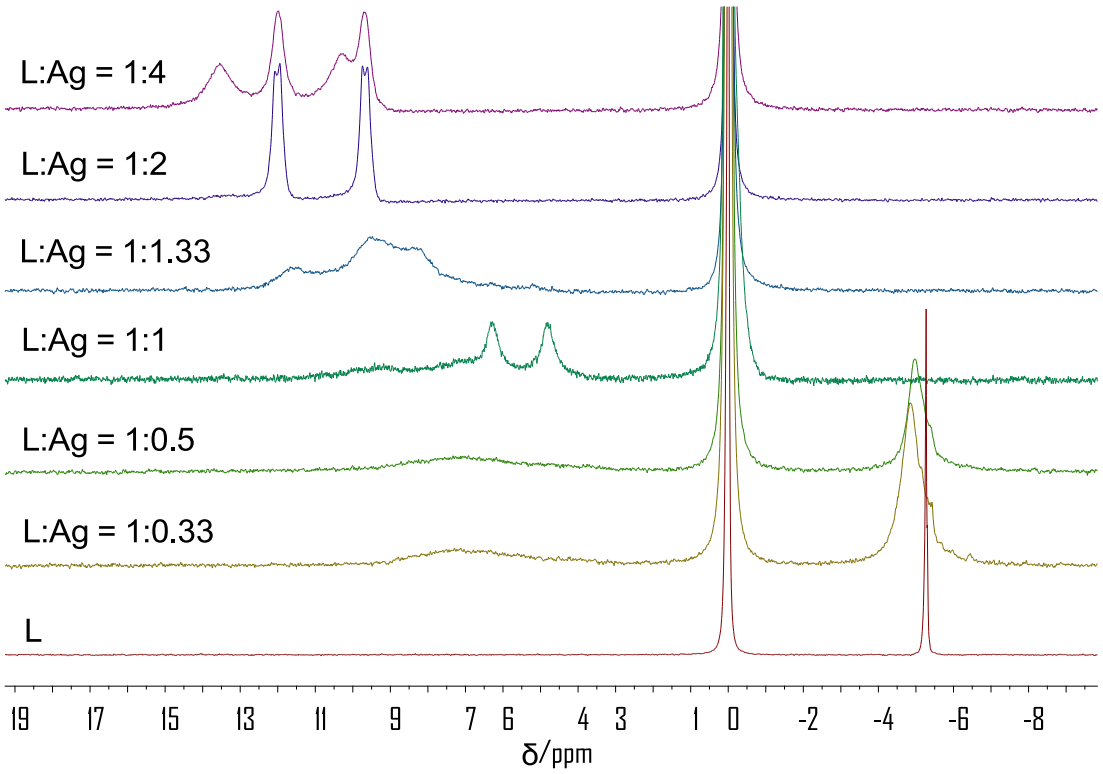

Fig. S9 $^{31}P\{^{1}H\}$ NMR titration of L with $AgBF_4$ ($CDCl_3$-MeCN, 202 MHz) (reference: 85% conc. H_3PO_4).

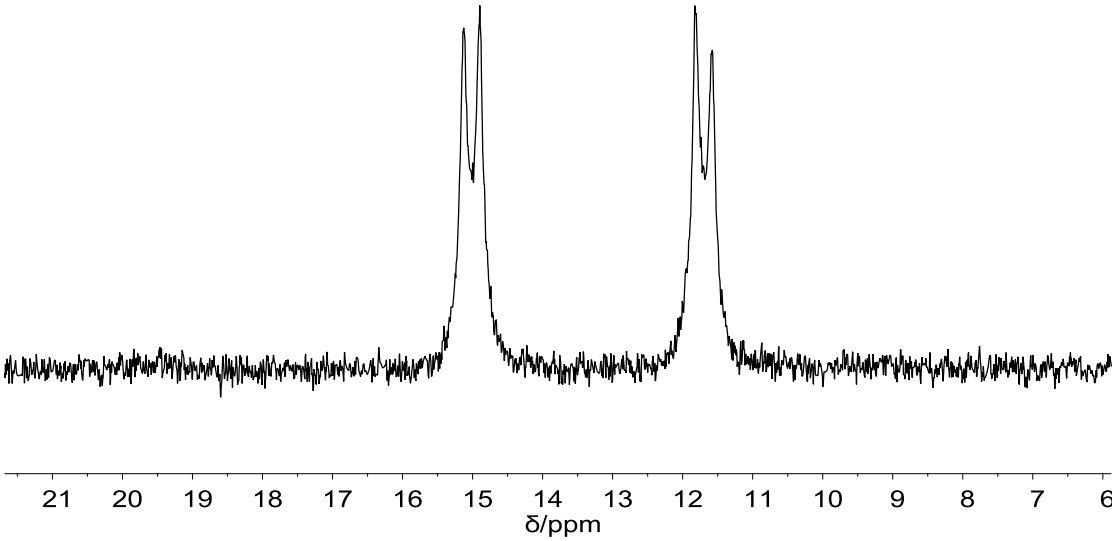

Fig. S10 $^{31}P\{^{1}H\}$ NMR spectrum (CD_2Cl_2, 162 MHz) of Ag_4L_2.

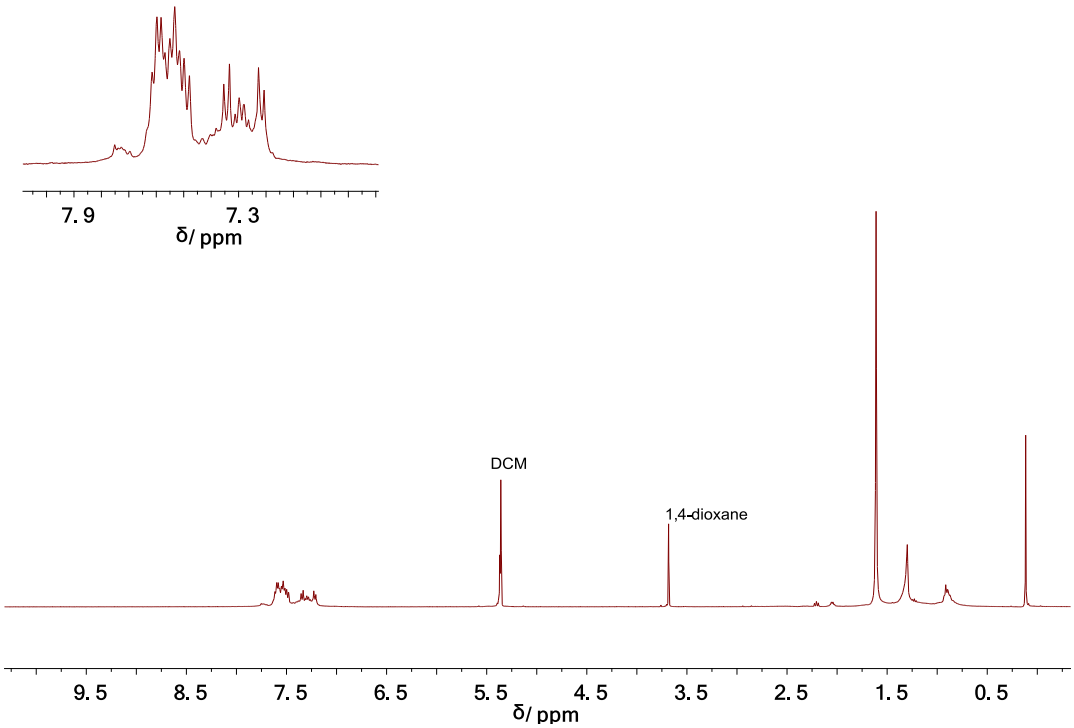

Fig. S11 ^{1}H NMR spectrum (CD_2Cl_2, 400 MHz) of Ag_4L_2.

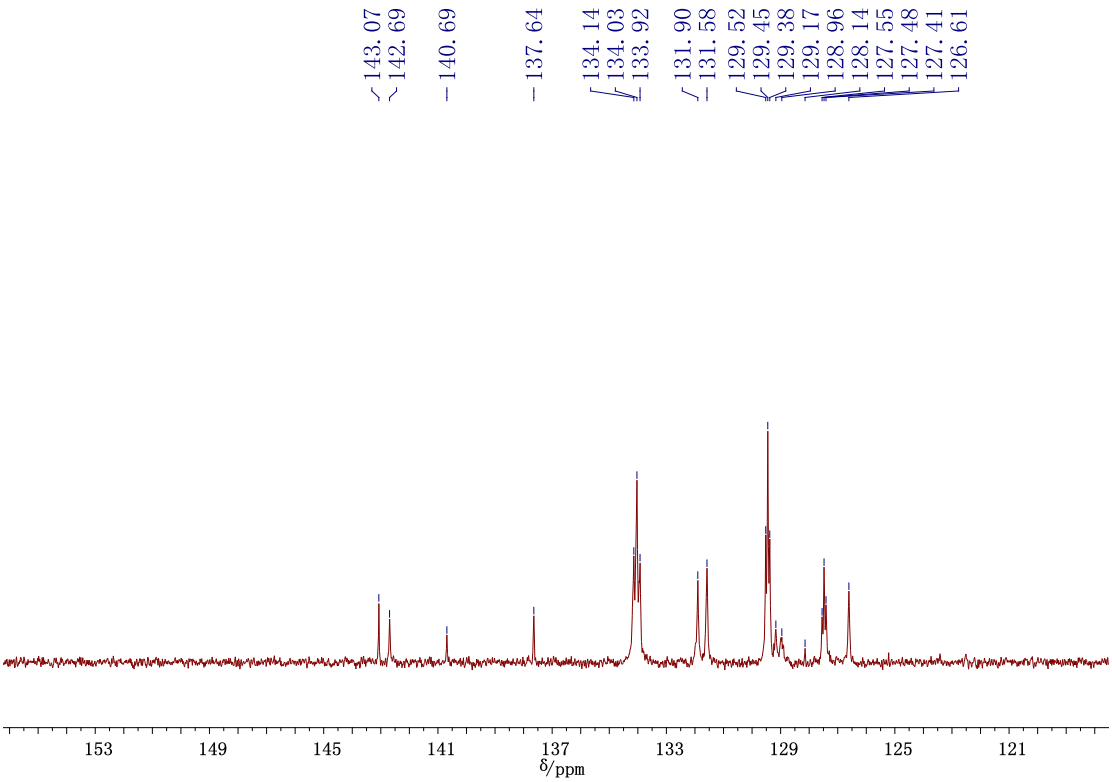

Fig. S12 ^{13}C NMR spectra (CD_2Cl_2, 75 MHz) of Ag_4L_2.

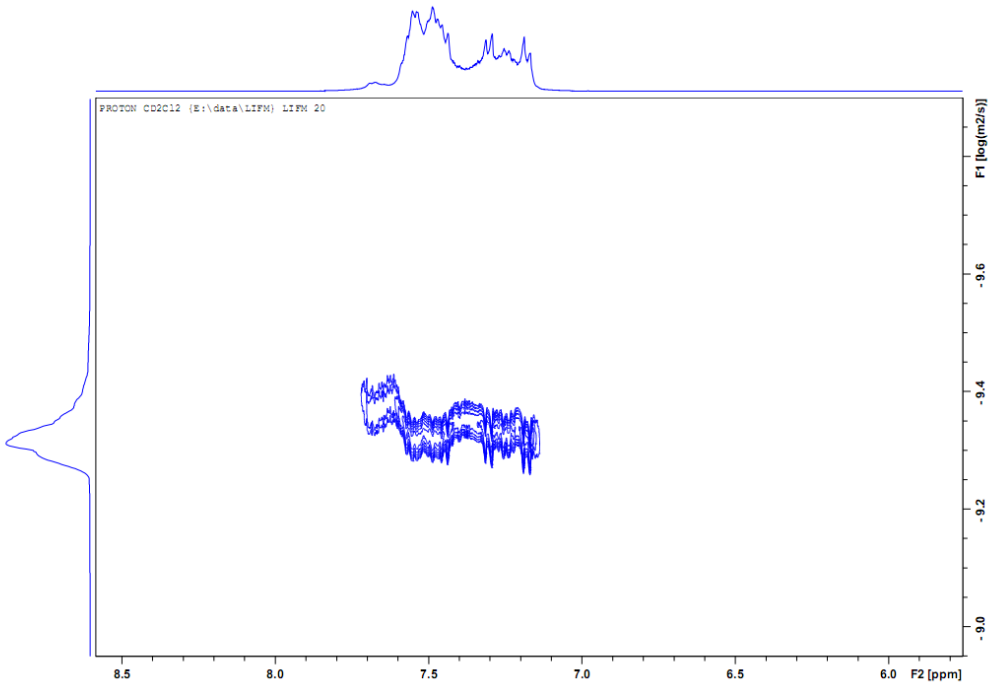

Fig. S13 Section of ^{1}H DOSY NMR spectrum (CD_2Cl_2, 400 MHz) of Ag_4L_2.

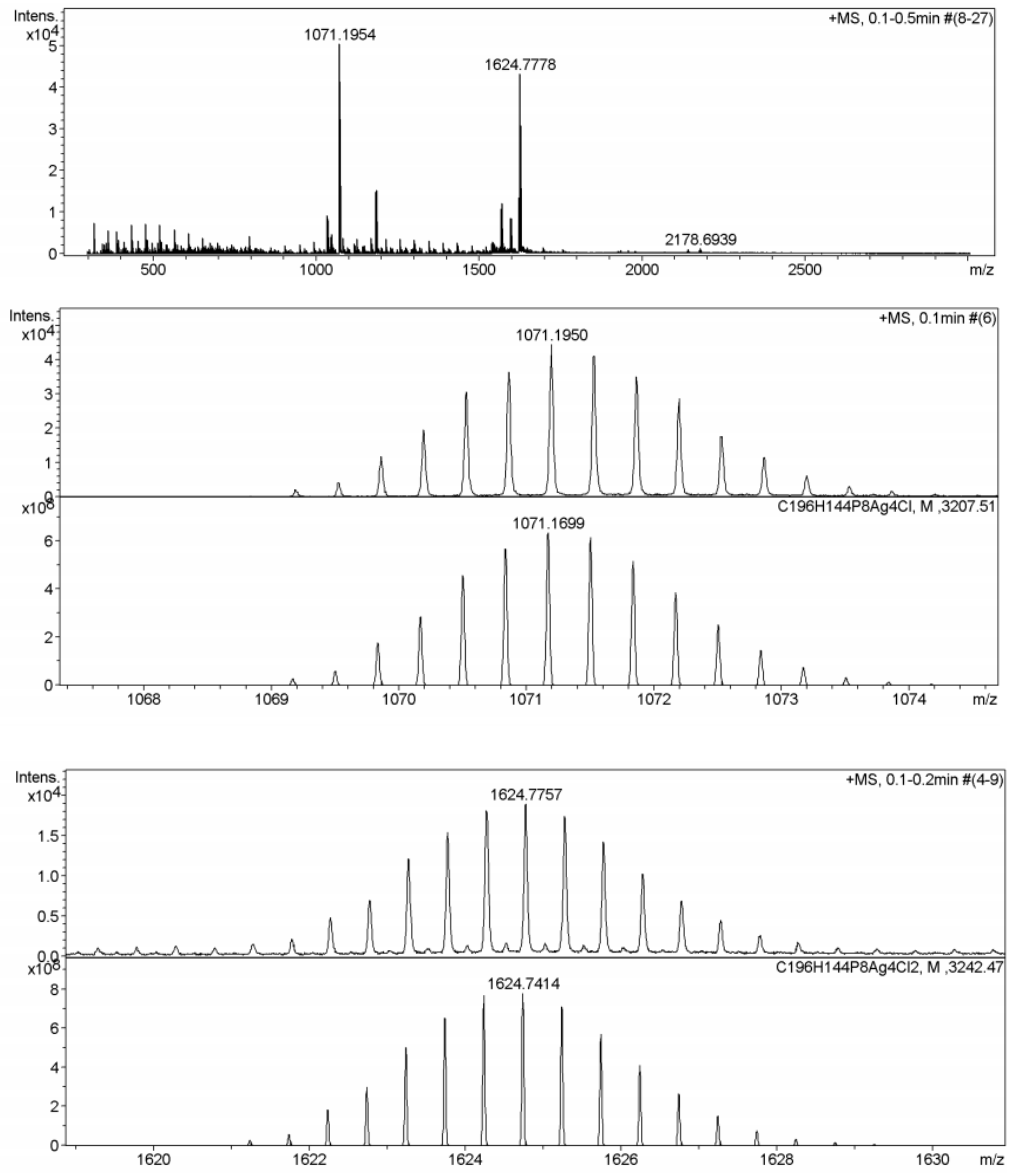

Fig. S14 ESI-TOF-MS spectrum of Ag_4L_2 in $CHCl_3$ (diluted by MeCN), and isotopic distributions and simulations of some key peaks. HRMS: *m*/*z* found (calcd) for $[Ag_4L_2+Cl]^{3+}$, 1071.1699 (1071.1796); $[Ag_4L_2+2Cl]^{2+}$, 1624.7775 (1624.7414).

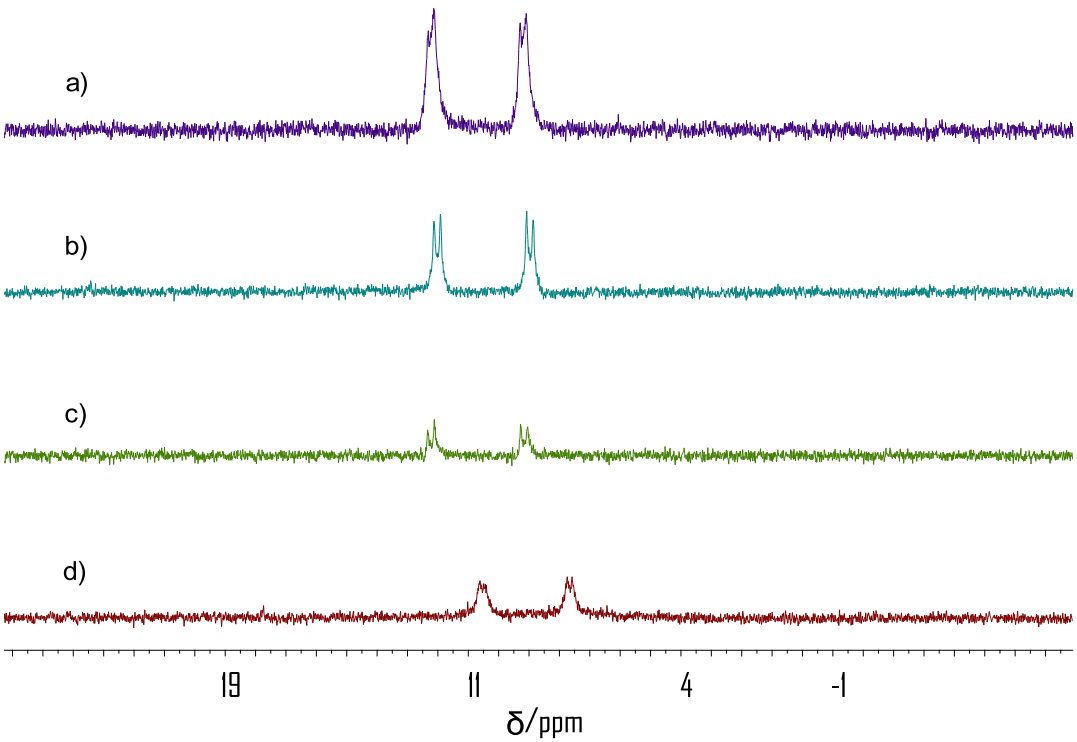

Fig. S15 $^{31}P\{^{1}H\}$ NMR (298 K, 162 MHz) spectra for mixtures of L and Ag^{+} with different anions (Ag:L = 2:1), a) NO_3^-; b) BF_4^-; c) SbF_6^- in toluene–methanol (v:v = 1:1), and d) OTf^- in CD_3CN.

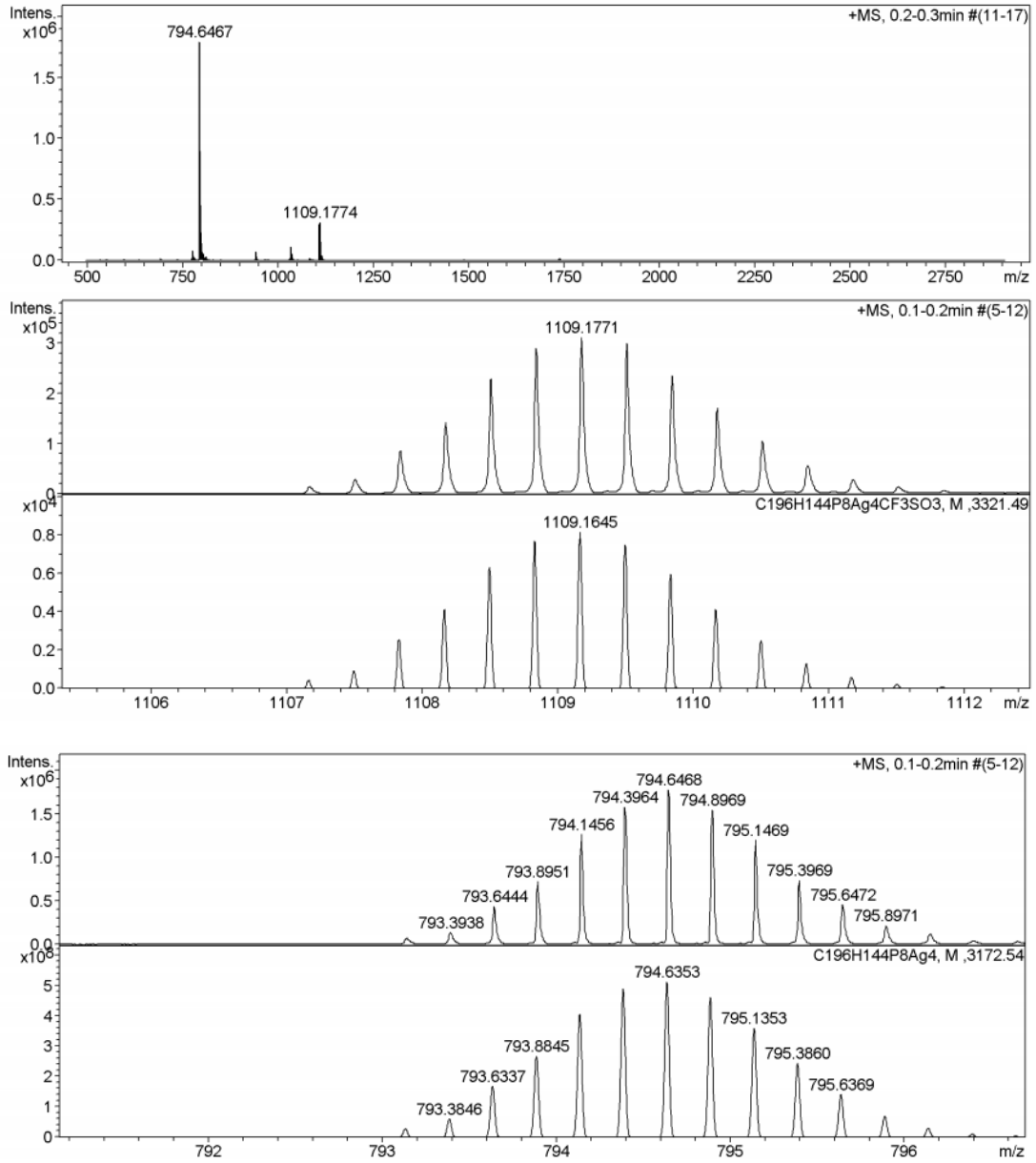

Fig. S16 ESI-TOF-MS spectrum of mixtures of L and AgOTf (L:Ag = 1:2) in toluene–methanol (v:v = 1:1). HRMS: *m*/*z* found (calcd.) for $[Ag_4L_2+OTf]^{3+}$, 1109.1771 (1109.1645); $[Ag_4L_2]^{4+}$, 794.6468 (794.6353).

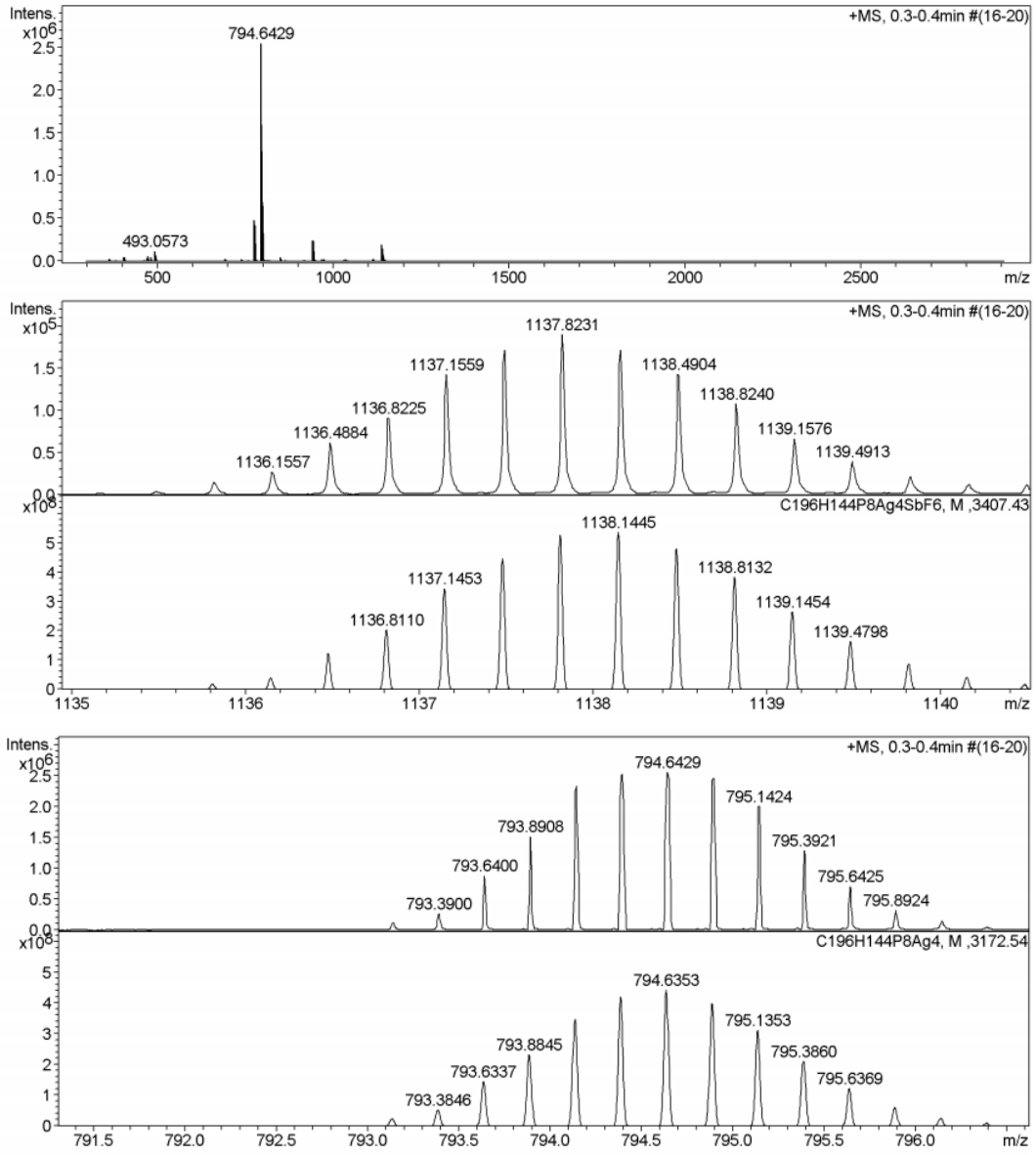

Fig. S17 ESI-TOF-MS spectrum of mixtures of L and $AgSbF_6$ (L:Ag = 1:2) in toluene–methanol (v:v = 1:1). HRMS: *m*/*z* found (calcd.) for $[Ag_4L_2+SbF_6]^{3+}$, 1137.8231 (1137.8118); $[Ag_4L_2]^{4+}$, 794.6429 (794.6353).

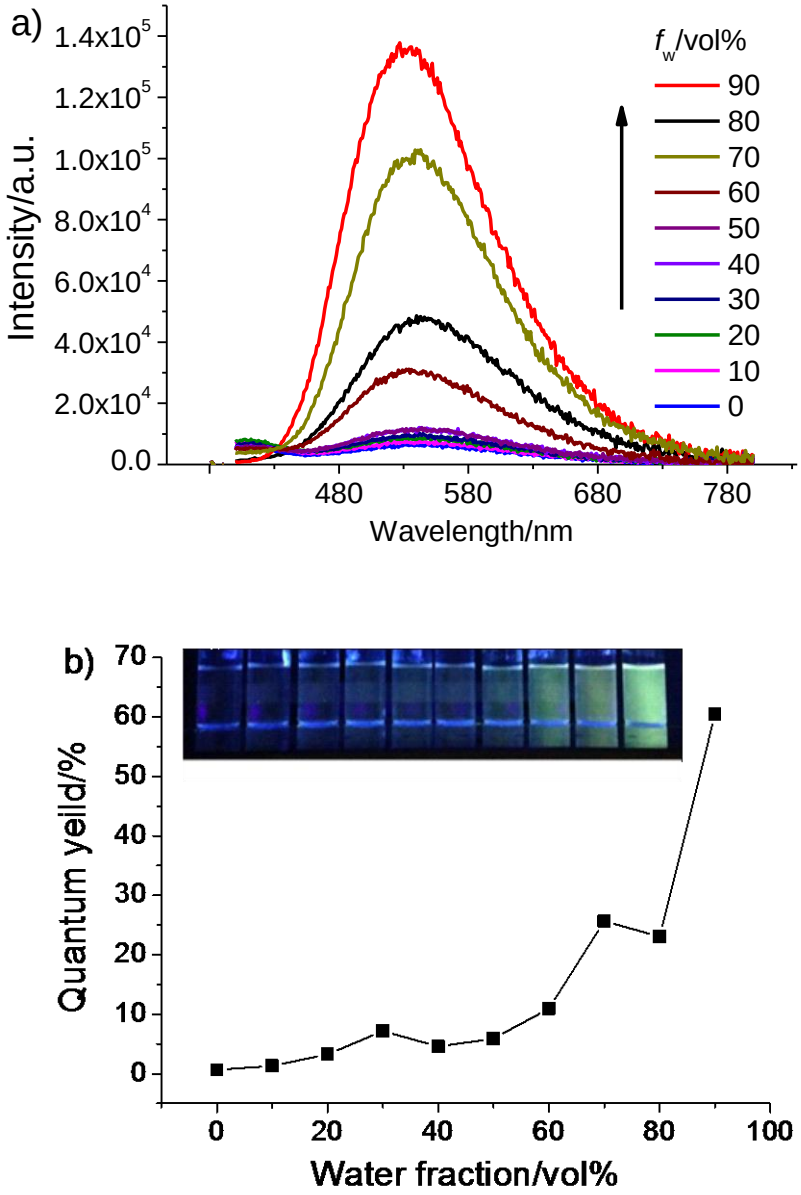

Fig. S18 a) Photoluminescence spectra of L in THF–water mixtures with different water fractions (f_w) and in pure THF (f_w = 0%). b) Variations of fluorescence quantum yields of L with water fractions in THF/water mixtures. c = 1.82 ×10^{-5} mol L^{-1}; λ_{ex} = 310 nm. Inset shows the photos of L in pure THF and THF-water mixtures taken under UV light (365 nm) (from left to right: 0 → 90% H_2O fraction/vol%).

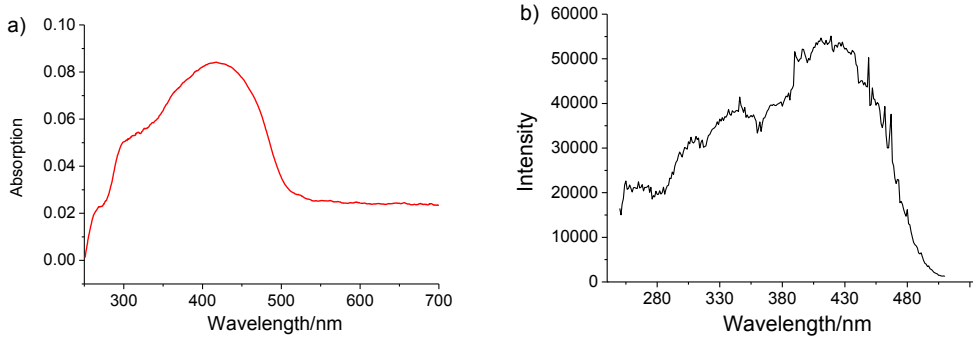

Fig. S19 a) UV-vis absorption spectrum of L in solid state and b) excitation spectrum of L in solid state (λ_{em} = 530 nm).

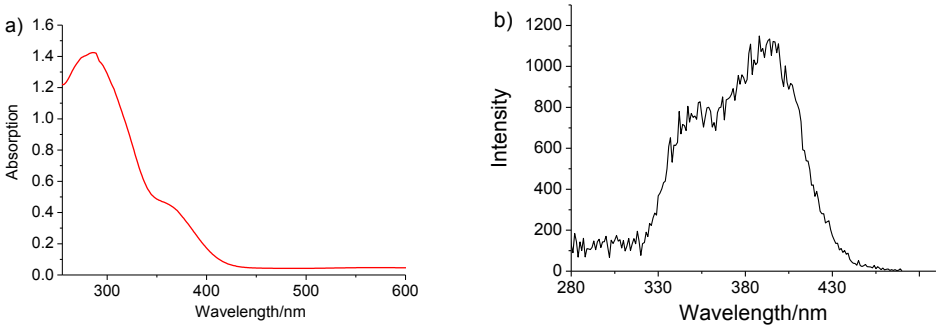

Fig. S20 a) UV-vis absorption and b) excitation spectra of L in $CHCl_3$ (c = 1.53×10^{-5} mol L^{-1}) (λ_{em} = 490 nm).

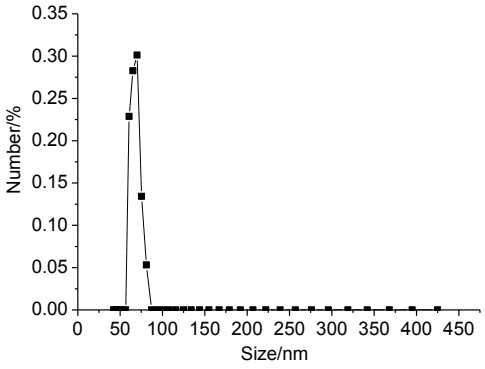

Fig. S21 Size distributions of L in THF-water mixture (f_w = 90%, c = 1.82×10^{-5} mol L^{-1}).

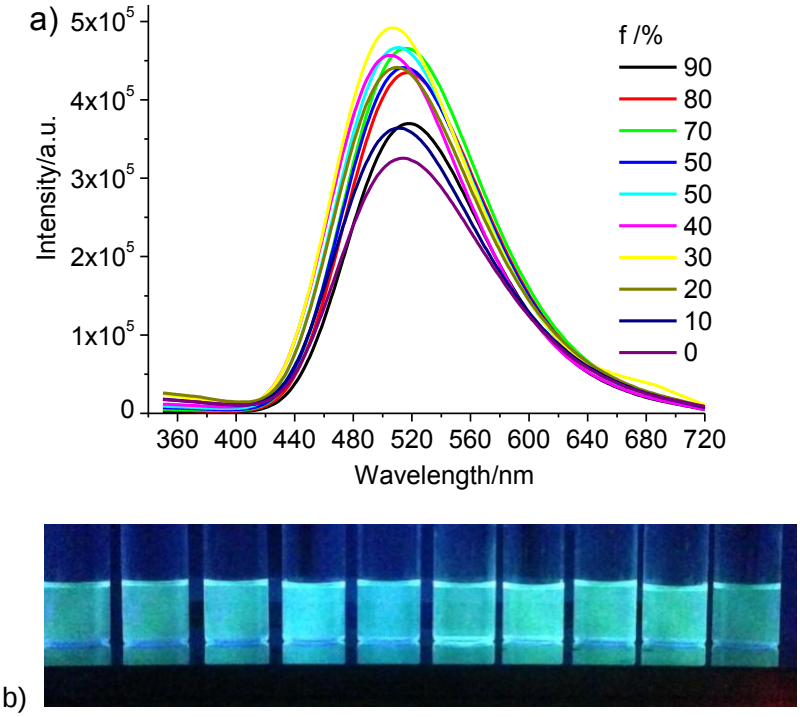

Fig. S22 a) Fluorescence emission spectra of Ag_4L_2 in CH_2Cl_2-hexane mixtures with the volume fractions of hexane (*f*) varying in the range of 0-90% (1.42×10^{-5} mol L^{-1}, λ_{ex} = 310 nm). b) Photos of Ag_4L_2 in pure CH_2Cl_2 and CH_2Cl_2-hexane mixtures taken under UV light (365 nm) (from left to right: 0 → 90% hexane fraction/vol%).

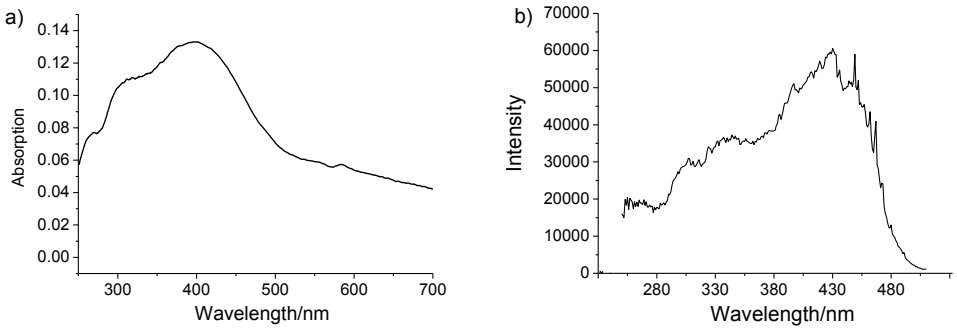

Fig. S23 a) UV-vis absorption spectrum of Ag_4L_2 in solid state and b) excitation spectrum of Ag_4L_2 in solid state (λ_{em} = 530 nm).

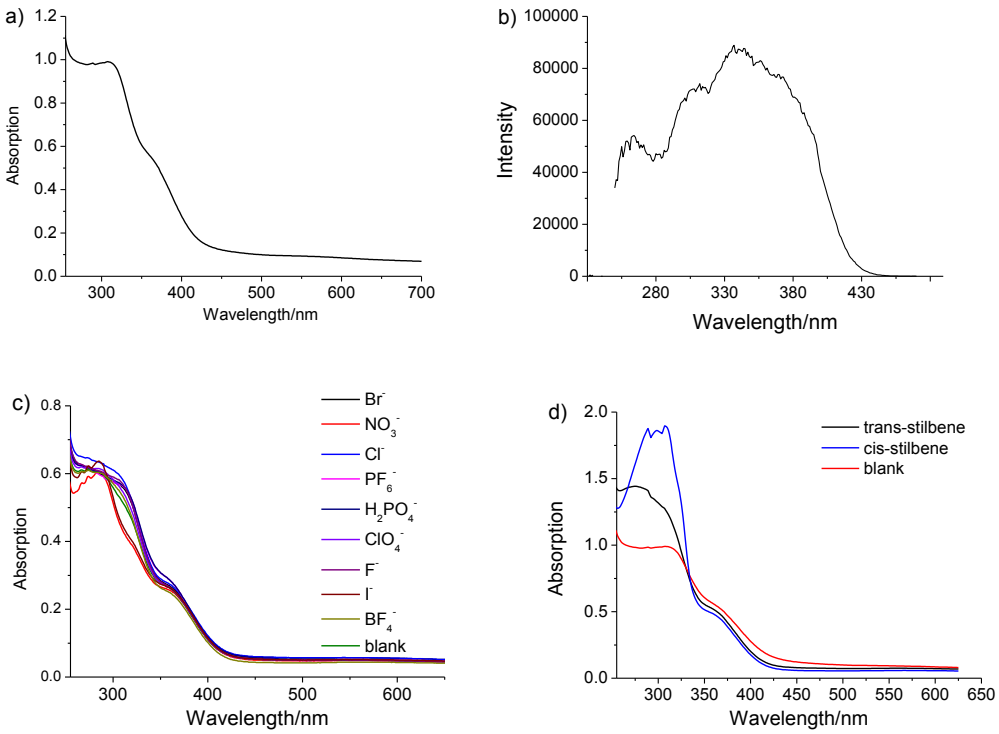

Fig. S24 a) UV-vis absorption and b) excitation spectra of Ag_4L_2 in $CHCl_3$ (c = 1.42×10^{-5} mol L^{-1}) (λ_{em} = 490 nm), c) UV-vis spectra of Ag_4L_2 in $CHCl_3$ (7.99×10^{-6} mol L^{-1}) in the presence of four equiv TBA salts of anions, d) UV-vis spectra of Ag_4L_2 in $CHCl_3$ (1.69×10^{-5} mol L^{-1}) in the presence of four equiv aromatic compounds, cis-stilbene, trans-stilbene and blank.

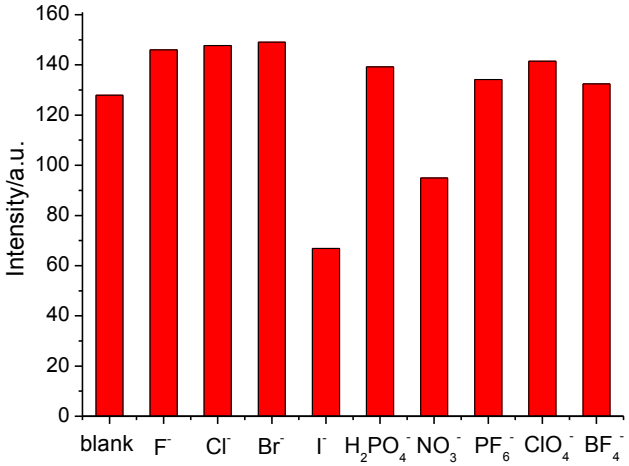

Fig. S25 Photoluminescence intensity upon addition of various TBA salts of anions of Ag_4L_2 in $CHCl_3$ (7.99×10^{-6} mol L^{-1}, λ_{ex} = 310 nm) in the presence of 4 equiv TBA salts of anions.

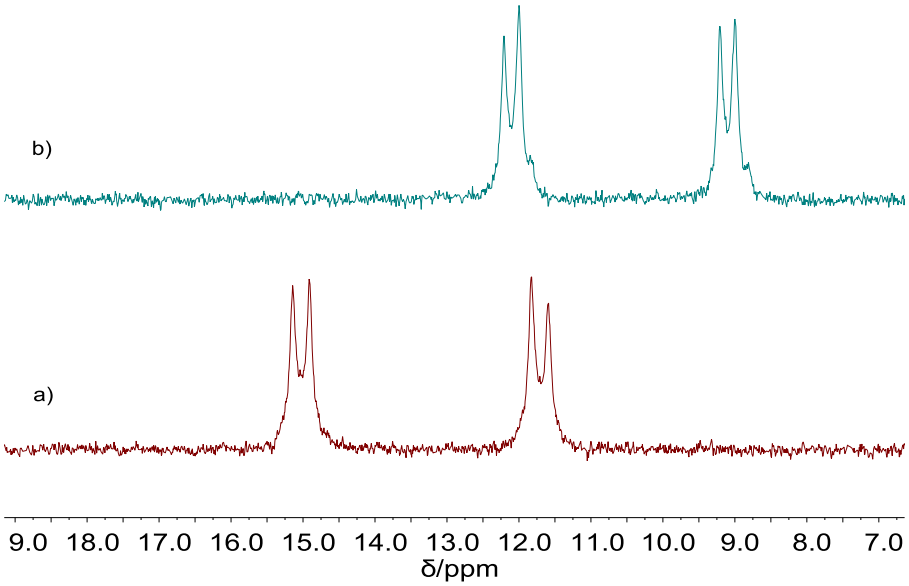

Fig. S26 $^{31}P\{^{1}H\}$ NMR spectrum (CD_2Cl_2, 162 MHz) of Ag_4L_2, a) blank ($J_{^{109}Ag-^{31}P}$ = 500 Hz), b) upon addition of excess NO_3NBu_4 ($J_{^{109}Ag-^{31}P}$ = 452 Hz).

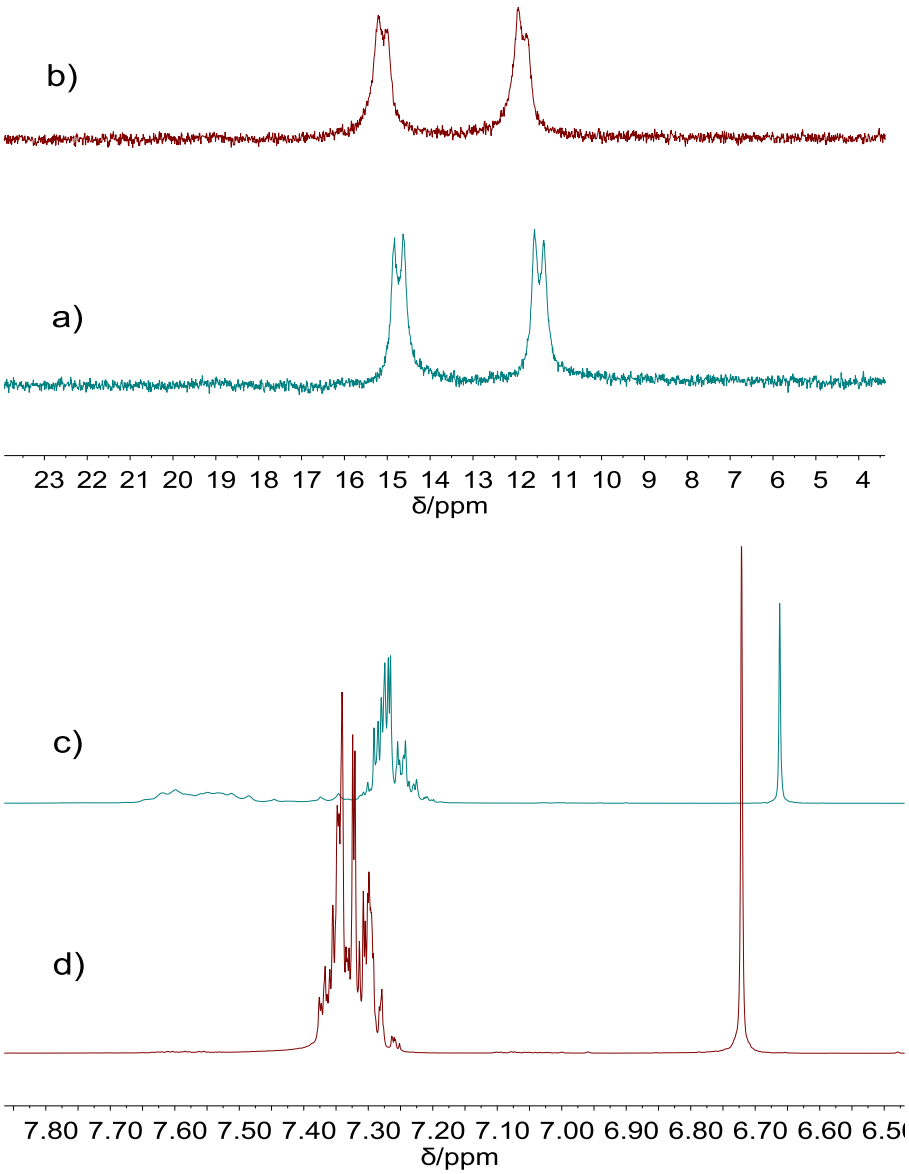

Fig. S27 $^{31}P\{^{1}H\}$ NMR spectrum (CD_2Cl_2, 162 MHz) (top) and ^{1}H NMR (CD_2Cl_2, room temperature, 400 MHz) (bottom) of Ag_4L_2, a) blank, b,c) upon addition of excess cis-stilbene (Note the olefin H change on the high field) and d) cis-stilbene.

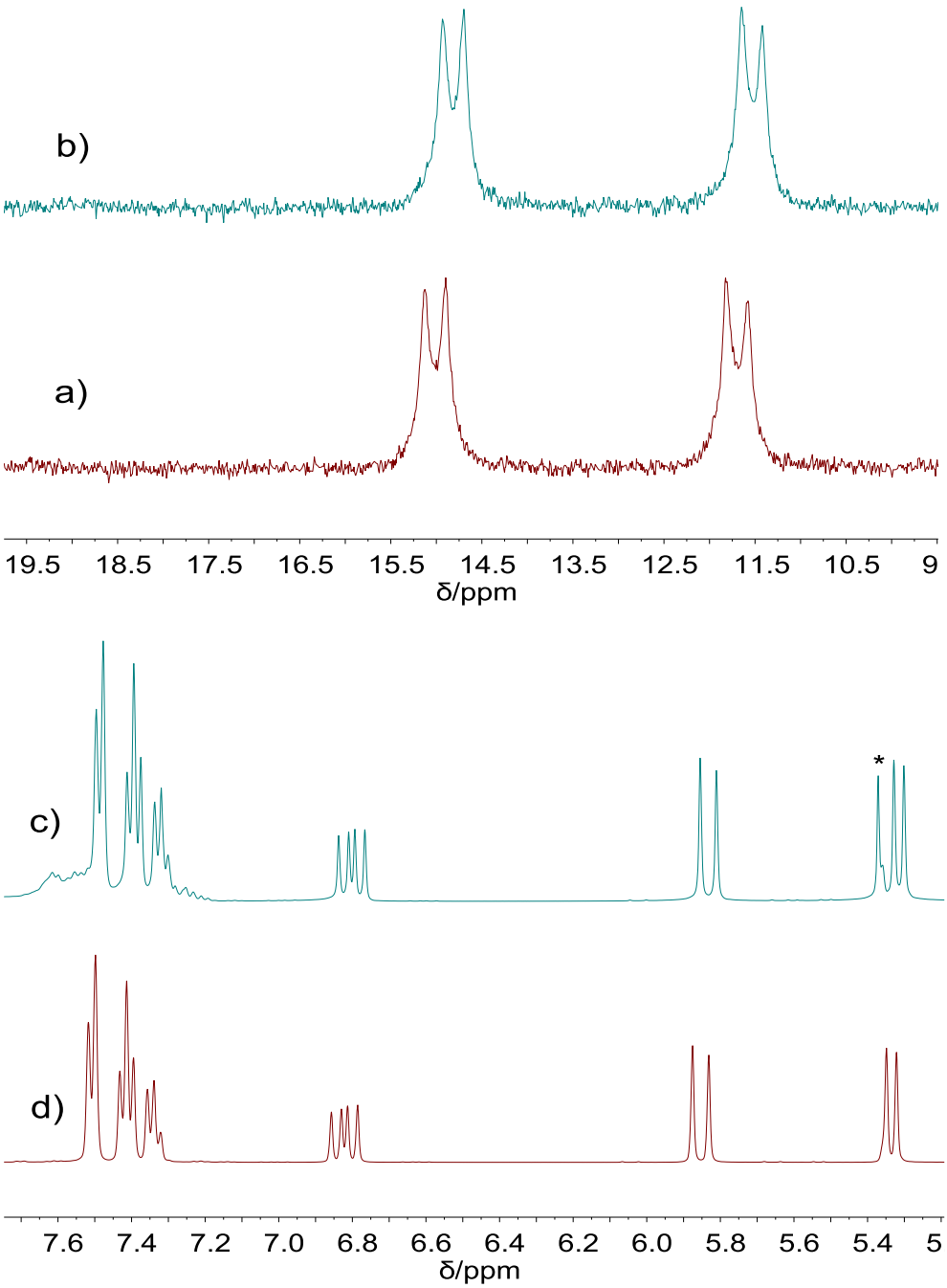

Fig. S28 $^{31}P\{^{1}H\}$ NMR spectrum (CD_2Cl_2, 162 MHz) (top) and ^{1}H NMR (CD_2Cl_2, room temperature, 400 MHz) (bottom) of Ag_4L_2, a) blank, b,c) upon addition of excess styrene (* is due to CD_2Cl_2) and d) styrene.

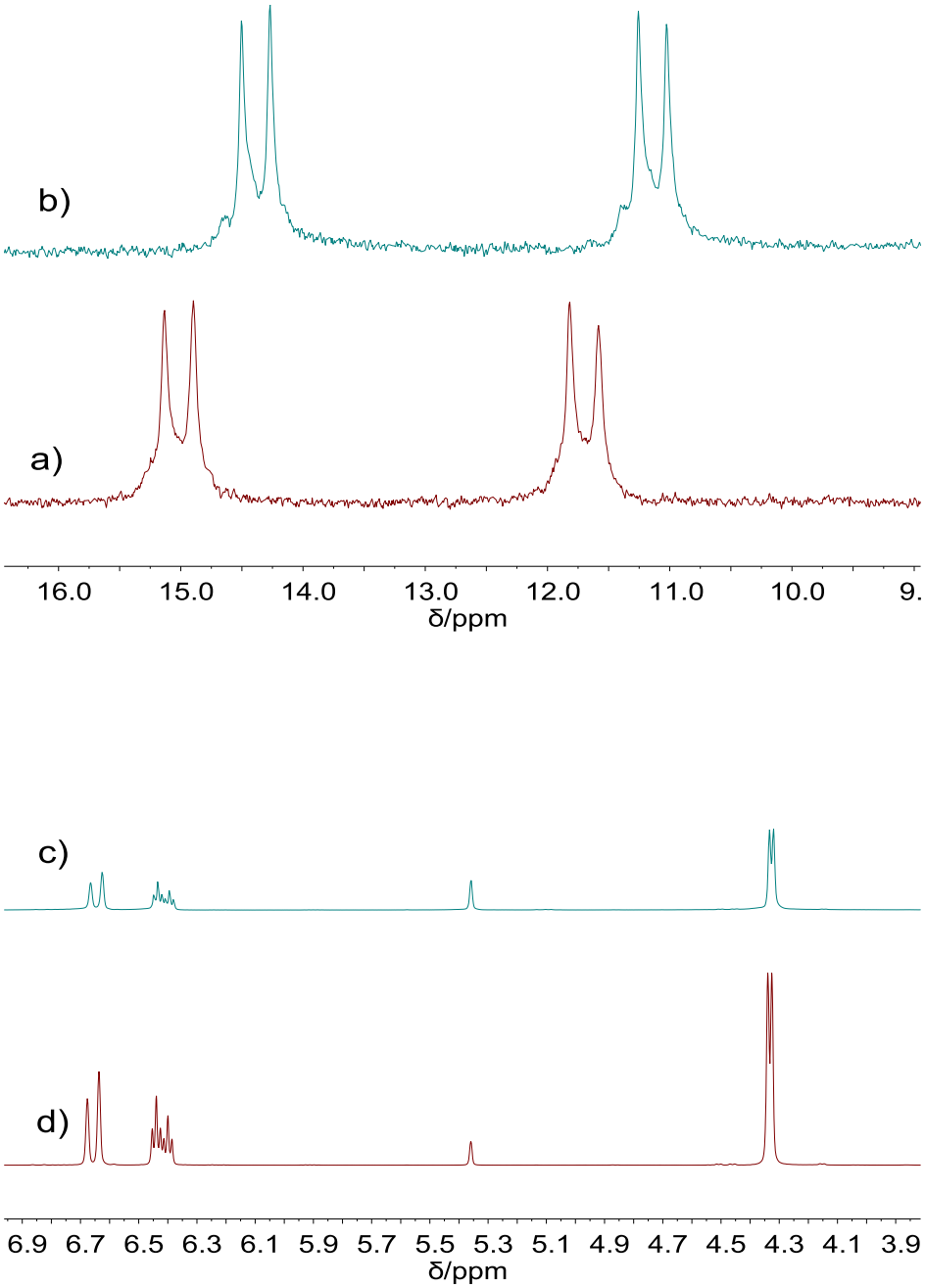

Fig. S29 $^{31}P\{^{1}H\}$ NMR spectrum (CD_2Cl_2, 162 MHz) (top) and ^{1}H NMR (CD_2Cl_2, room temperature, 400 MHz) (bottom) of Ag_4L_2, a) blank, b,c) upon addition of excess cinnamyl alcohol, and d) cinnamyl alcohol. The NMR change is probably due to the Ag…OH(alcohol) interaction.

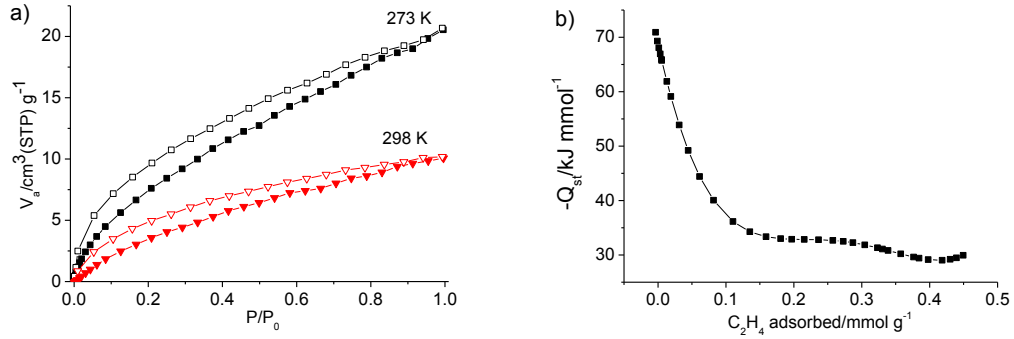

Fig. S30 a) C_2H_4 sorption isotherms of Ag_4L_2 at 273 and 298 K (filled, adsorption; unfilled, desorption), and b) The isosteric heat of adsorption, Q_{st} of C_2H_4.